Electronic Supplementary Information

Ullmann-Type Coupling of Brominated Tetrathienoanthracene on Copper and Silver

Rico Gutzler, Luis Cardenas, Josh Lipton-Duffin, Mohamed El Garah, Laurentiu E. Dinca, Csaba E. Szakacs, Chaoying Fu, Mark Gallagher, Martin Vondráček, Maksym Rybachuk, Dmitrii F. Perepichka, and Federico Rosei

DFT Calculations

The Gaussian09 software suite[1] was used to perform gas-phase DFT calculations. Single TBTTA molecules as well as polymers with different structure were modelled under periodic boundary conditions (PBC). Geometry optimization was performed using the M06-L functional[2] together with the 6-31G basis set. All atomic positions were allowed to freely relax in the three spatial dimensions, repeatedly yielding flat geometries of TBTTA and its organometallic networks and polymers. Lattice vectors were free to relax in PBC calculations.

The two observed networks have been calculated as 2D polymers or organometallic networks and their size compared to the experimental values. The dominant ordered structures that are encountered in STM images either have an oblique unit cell or correspond to a Kagome lattice. The unit cell of the oblique structure measures 1.21 nm × 1.21 nm with an angle of 109.4° in the 2D polymer (Fig. S1a). For the copper-coordinated organometallic network of similar geometry the unit cell measures 1.45 nm × 1.45 nm, 103.1° and for the Ag-coordinated network 1.49 nm × 1.49 nm, 102.6° (Fig. S1b). The Kagome polymer is built from a hexagonal unit cell of 2.21 nm × 2.21 nm, 120.0°, while the organometallic analogue measures 2.70 nm × 2.70 nm, 120.0° (Fig. S1c,d). The calculated sizes of polymeric *vs.* organometallic structures allow the unambiguous assignment of which is observed in STM images.

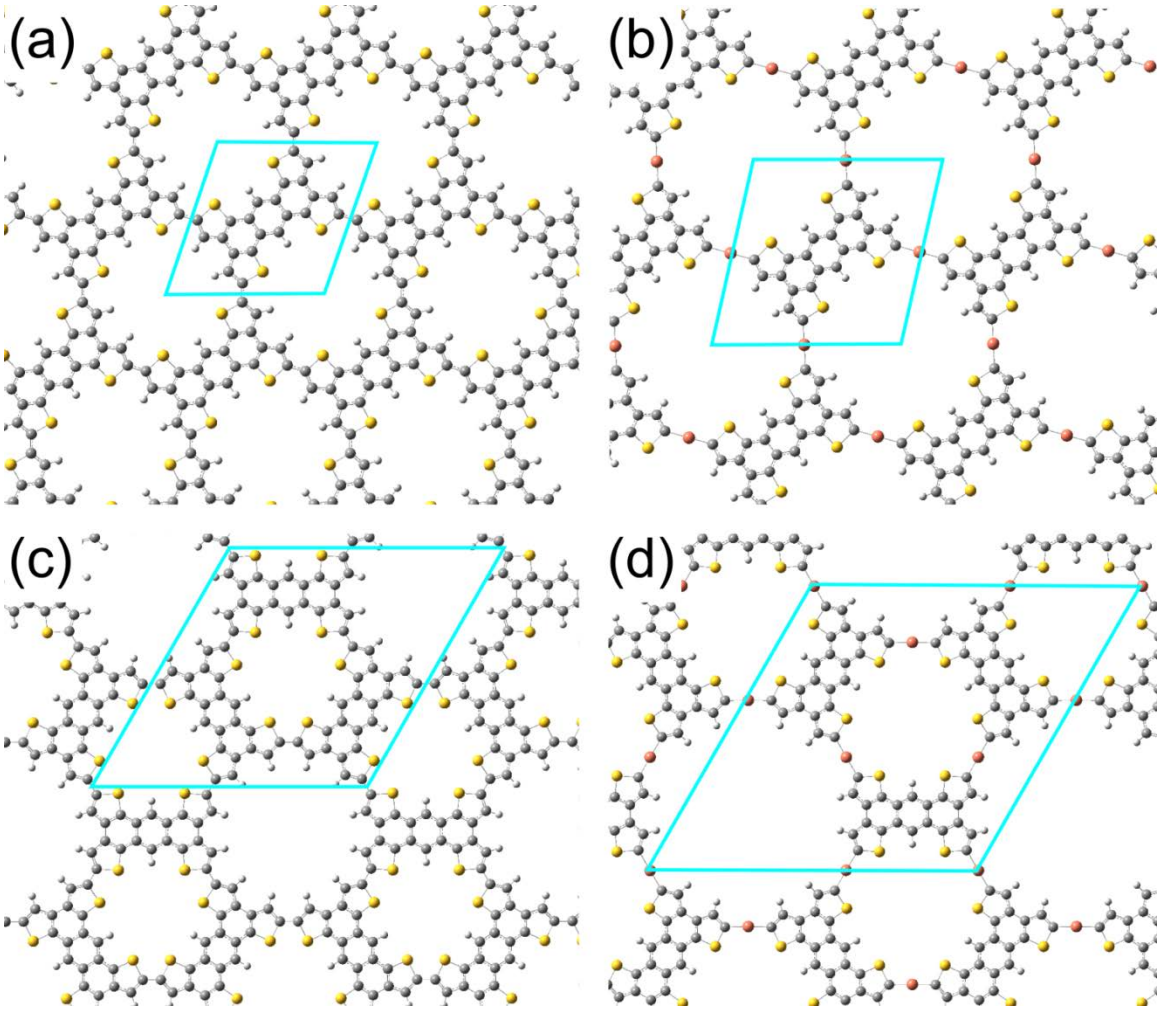

Figure S1. (a) Oblique 2D covalent polymer. (b) Oblique organometallic network. (c) Kagome 2D covalent polymer. (d) Kagome organometallic network. Unit cells are given in blue.

To assess the chemical shifts in the sulfur S 2p core-level assigned to C−C−S vs. Ag−C−S bonding environments in covalent polymeric and organometallic networks, we performed Natural Bond Orbital calculations[3] as implemented in the Gaussian09 software suit (M06L functional and 6-31G* basis set for carbon, sulphur, bromine and hydrogen, and the LanL2DZ basis set for silver). This approach gives direct access to core level energies, which were calculated for three different clusters (Figure S2).

The calculated S 2p binding energies are (on average) 158.62 eV in cluster **I**, 158.39 eV in cluster **II**, and 157.29 eV in cluster **III**. Comparing energies in **II** and **III** shows a shift in the S 2p level of ~1 eV to lower energy from covalent to organometallic network. In the XPS experiments we observed a shift of 0.5 eV to lower binding energy, in qualitative agreement with our calculation.

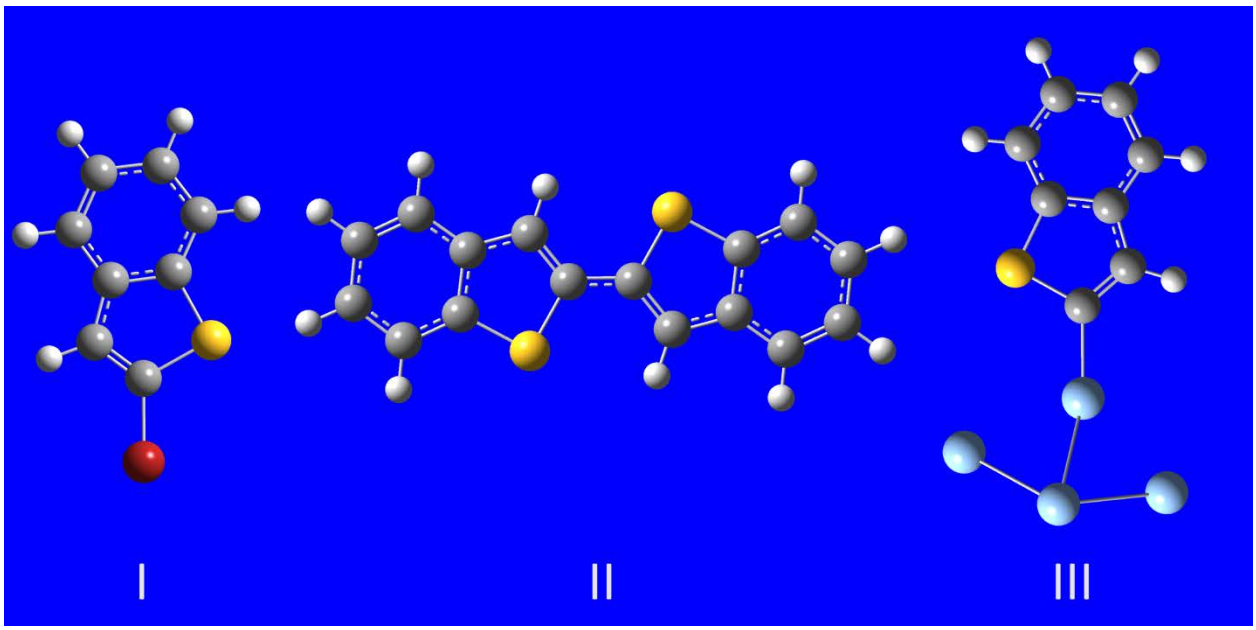

Figure S2. Optimized geometries of three different clusters. **I** fragment of the intact TBTTA molecule. **II** fragment of the covalent network. **III** fragment of the organometallic network.

DFT calculations taking into consideration the silver substrate were performed within the local density approximation. All the optimizations employed the Perdew-Zunger exchange-correlation energy functional[4] and norm-conserving pseudo potentials as implemented in the SIESTA package.[5] The Ag(110) surface was modelled using a 5 × 5 unit cell, with a slab comprising three layers of Ag atoms. A sufficiently large (~2 nm) vacuum layer was included in the *z*-direction in order to avoid possible artificial interactions between the periodic slabs. During the optimization the two bottom layers were kept fixed, while the surface was relaxed. The number of layers has been found to be sufficiently large to represent the Ag(110) surface structure. Planar adsorption sites of the TTA at different positions and orientations on the Ag(110) surface were considered. The total energy of each TTA/Ag(110) geometry conformation was calculated and the minimum energy structure was thereby determined. In all calculations the energy minimization was achieved employing an algorithm based on the conjugate-gradient optimization method. Tight convergence for the plane wave expansion was obtained using a kinetic energy cut-off of 400 Ry.

In contrast to the organometallic Kagome network in which copper adatoms are coordinated by TTA molecules (*cf.* Fig. 1), the organometallic structure on Ag(110) seems not to be stabilized by adatoms. The debrominated molecules bond directly to silver atoms that constitute the surface. STM images with atomic resolution of the surface as well as the molecular layer of structure **II** (Fig. S3a) allow for the measurement of the exact size and orientation of its unit cell. The epitaxial relation between molecular suprastructure and silver surface is described by the epitaxy matrix (−3, 4 | 2, −2). In Fig. S3b, a model of the molecule is overlaid over an STM image with molecular resolution. Bright circular protrusions are observed between molecular chains that form along the [1−11] direction. These might be attributed to atomic bromine adsorbed on the surface. The stoichiometric ratio is two circular protrusions per butterfly shaped TTA molecule. The information acquired from the experimental orientation of the molecule was used as input for DFT calculations that include the surface (performed with the SIESTA code). Fig. S3c is a model of the structure of dehalogenated TTA on Ag(110), in which the optimized adsorption geometry of the molecule agrees with experiment. From this model we infer that the bright circular protrusions are positioned on on-top sites and attribute them to either bromine, Ag adatoms, or possibly Br−Ag clusters.

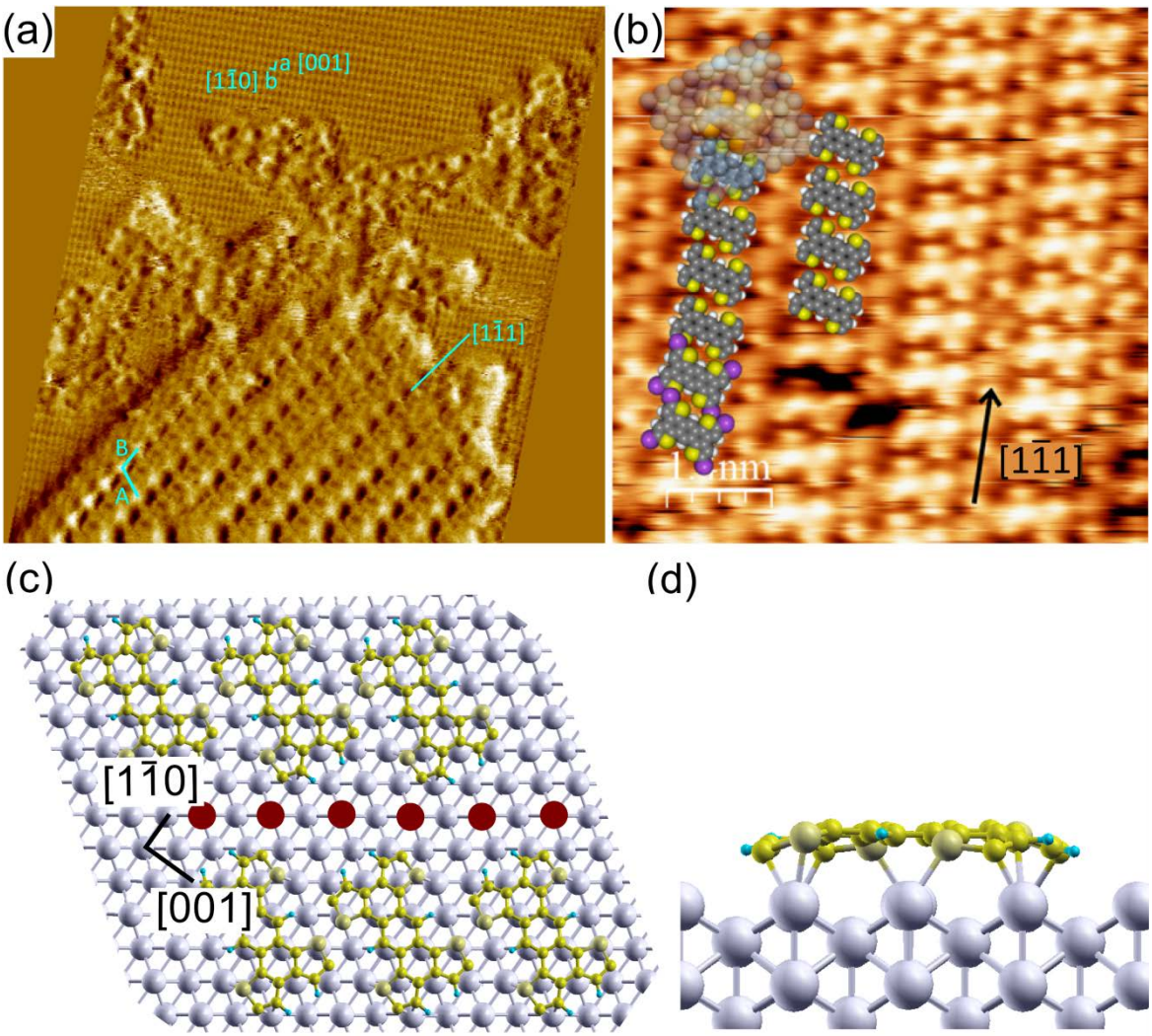

Figure S3. (a) STM topograph of Structure **II** with atomic resolution of the bare Ag(110) surface. (b) Structure **II** with overlaid molecular model. Brominated molecules (lower left structures, bromine in violet) are fairly large and substantial overlap between Br and neighboring molecules precludes intact TBTTA molecules as the building blocks of Structure **II**. (c) Composition of the DFT optimized structure with adsorbed bromine on expected adsorption sites. (d) Side view of (c). The terminal carbon atoms of the thiophene rings bend towards the surface in the formation of organometallic bonds with surface silver atoms.

Additional XPS Data

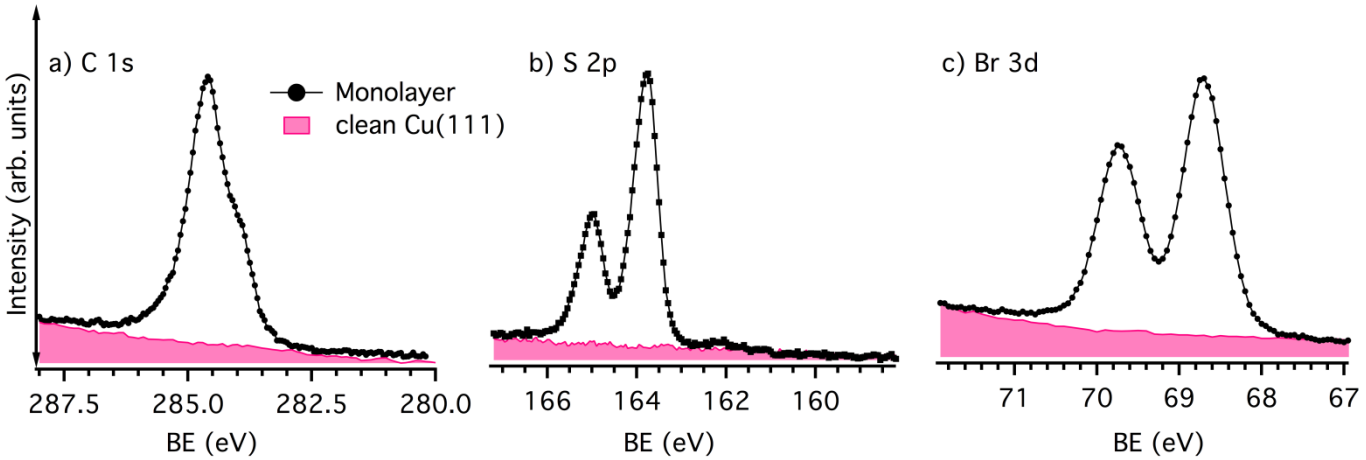

Figure S4. Photoelectron spectra on clean Cu(111) substrate (pink) and after deposition of ~1 monolayer of TBTTA (black curves). No carbon or sulfur impurities are observed on the clean copper surface.

Additional STM Data

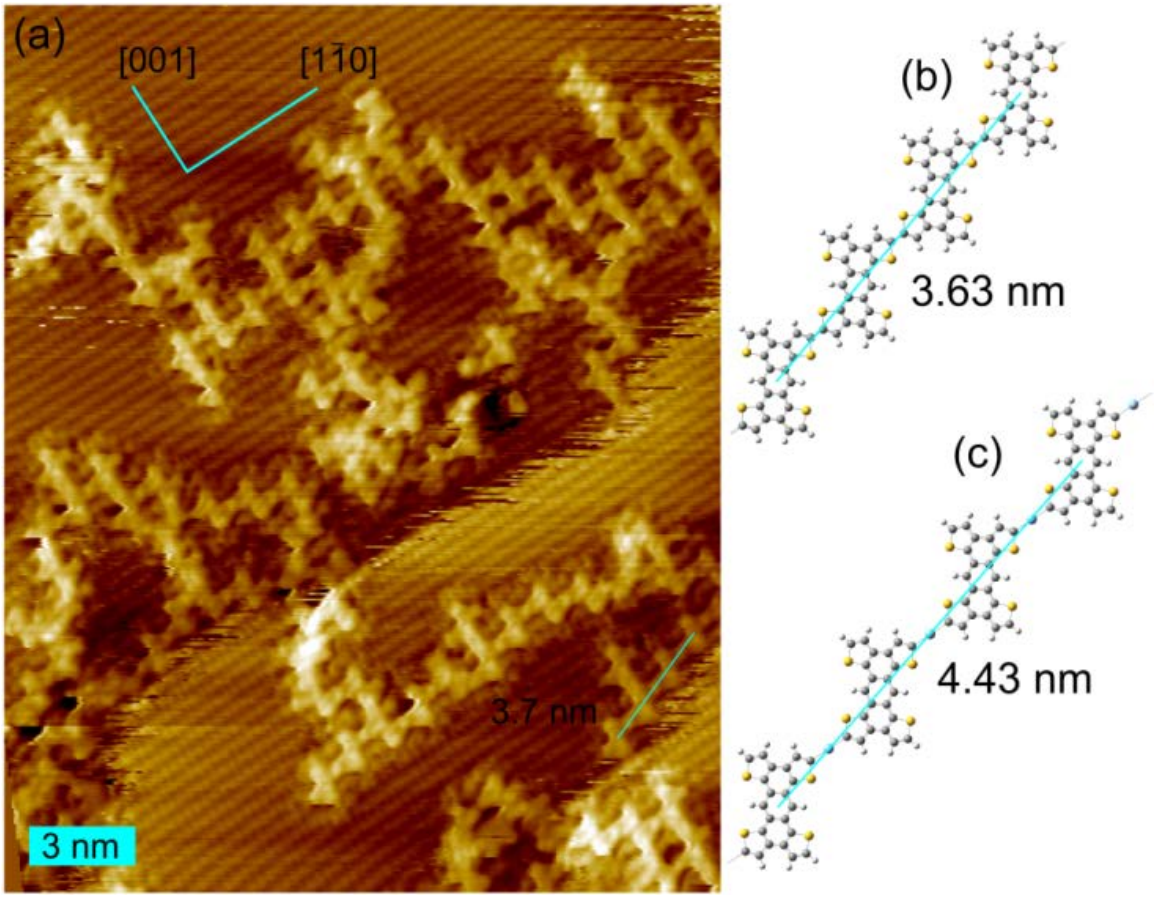

Figure S5. STM image of polymeric molecular structures together with atomic resolution of the Ag(110) substrate (U_{bias} = −760 mV, I_{tunnel} = 0.5 nA). The distance between the cores of four molecules in a linear oligomer to the right of the topography measures 3.7 nm, resulting in a distance of 1.2 nm between two adjacent molecules. DFT calculations yield a distance of 3.63 nm between four units of a 1D polymer chain (b), coupled through C−C bonds at the former C−Br sties. Organometallic structures can be excluded since the distance is increased by more than 20% with respect to the polymer, well within the resolution of STM. The distance between four units in a hypothetical 1D organometallic chain in which TTA molecules coordinate Ag metal atoms is 4.43 nm, 0.8 nm larger than in the polymer and 0.7 nm larger than the distance measured in the STM image.

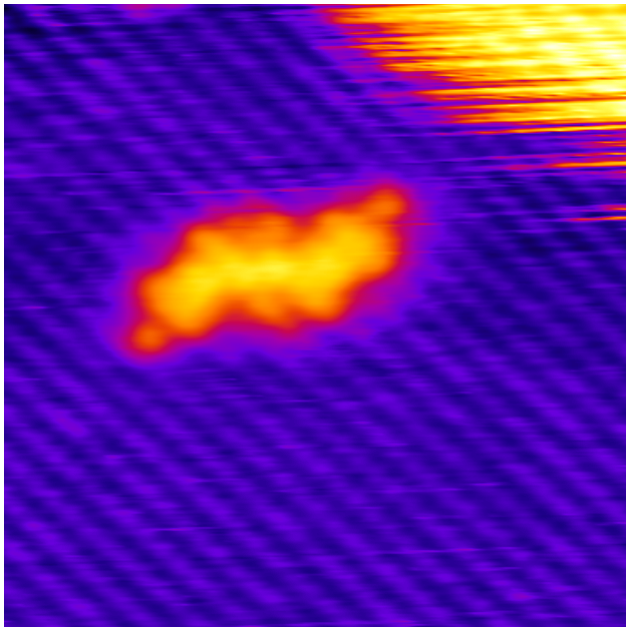

Figure S6. Same STM image as Fig. 8a after filtering. The Cu(110) lattice is atomically resolved.

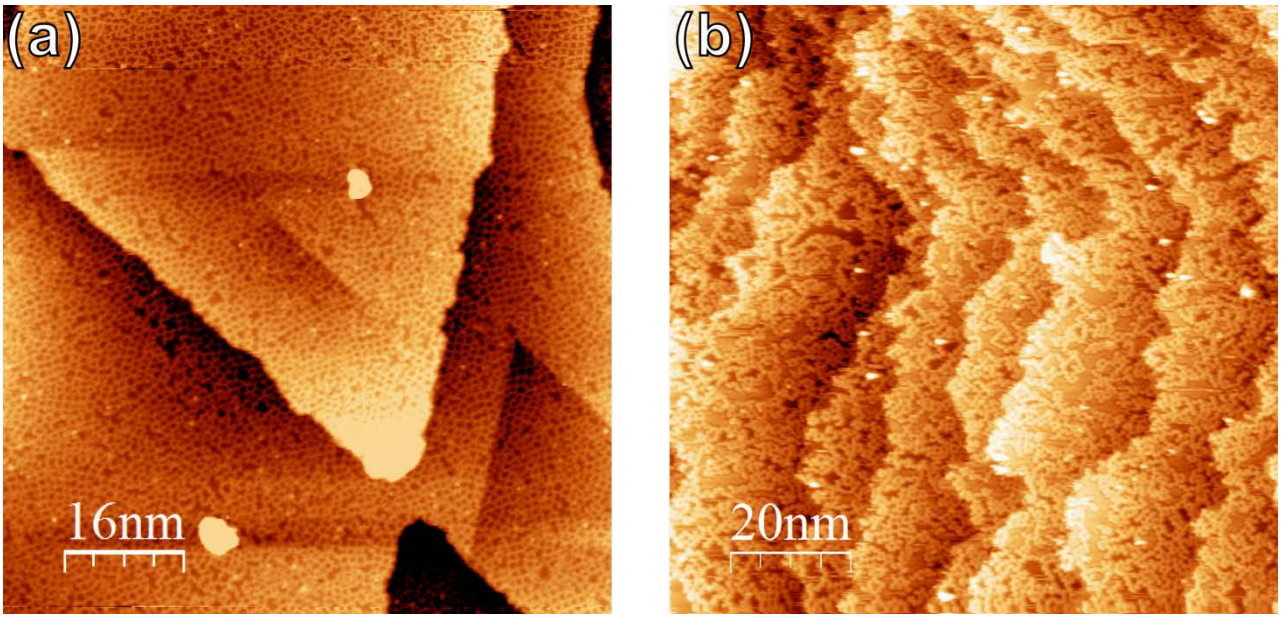

Figure S7. Large-scale STM image of the organic network after annealing to 300 °C on (a) Ag(111) and (b) Ag(110).

Bibliography

(1) Frisch, M. J.; Trucks, G. W.; Schlegel, H. B.; Scuseria, G. E.; Robb, M. A.; Cheeseman, J. R.; Scalmani, G.; Barone, V.; Mennucci, B.; Petersson, G. A.; Nakatsuji, H.; Caricato, M.; Li, X.; Hratchian, H. P.; Izmaylov, A. F.; Bloino, J.; Zheng, G.; Sonnenberg, J. L.; Hada, M.; Ehara, M.; Toyota, K.; Fukuda, R.; Hasegawa, J.; Ishida, M.; Nakajima, T.; Honda, Y.; Kitao, O.; Nakai, H.; Vreven, T.; Montgomery Jr., J. A.; Peralta, J. E.; Ogliaro, F.; Bearpark, M.; Heyd, J. J.; Brothers, E.; Kudin, K. N.; Staroverov, V. N.; Kobayashi, R.; Normand, J.; Raghavachari, K.; Rendell, A.; Burant, J. C.; Iyengar, S. S.; Tomasi, J.; Cossi, M.; Rega, N.; Millam, J. M.; Klene, M.; Knox, J. E.; Cross, J. B.; Bakken, V.; Adamo, C.; Jaramillo, J.; Gomperts, R.; Stratmann, R. E.; Yazyev, O.; Austin, A. J.; Cammi, R.; Pomelli, C.; Ochterski, J. W.; Martin, R. L.; Morokuma, K.; Zakrzewski, V. G.; Voth, G. A.; Salvador, P.; Dannenberg, J. J.; Dapprich, S.; Daniels, A. D.; Farkas, Ö.; Foresman, J. B.; Ortiz, J. V; Cioslowski, J.; Fox, D. J. *Gaussian 09, Revision B.01, Gaussian, Inc., Wallingford CT* **2009**.

(2) Zhao, Y.; Truhlar, D. G. *Acc. Chem. Res.* **2008**, *41*, 157–167.

(3) Glendening, E. D., Reed, A. E., Carpenter, J. E., Weinhold, F. *NBO Version 3.1*.

(4) Perdew, J. P.; Zunger, A. *Phys. Rev. B* **1981**, *23*, 5048–5079.

(5) Soler, J. M.; Artacho, E.; Gale, J. D.; García, A.; Junquera, J.; Ordejón, P.; Sánchez-Portal, D. *J. Phys. Condens. Matter* **2002**, *14*, 2745–2779.